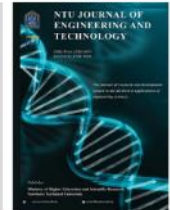




P-ISSN: 2788-9971 E-ISSN: 2788-998X

NTU Journal of Engineering and Technology

Available online at: <https://journals.ntu.edu.iq/index.php/NTU-JET/index>



Design, Modeling, and Comprehensive Analysis for The Wing of an Aircraft

Hakam Waadallah Shehab¹ , Mohammed Saleh Mohammed¹ , Mohammed Najeeb
Abdullah¹ 

¹Mechanical Engineering Department, College of Engineering, University of Mosul, Mosul, Iraq
hakam.22enp67@student.uomosul.edu.iq, moh62sam@uomosul.edu.iq, moh_77@uomosul.edu.iq

Article Informations

Received: 20-10-2024,
Revised: 24-12-2024,
Accepted: 10-02-2025,
Published online: 22-03-2025

Corresponding author:

Name: Hakam W. Shehab
Affiliation : University of
Mosul
Email:
hakam.22enp67@student.uomosul.edu.iq

Key Words:

wing design,
Stress Analysis,
Deformation,
Modeling,
load distribution,

ABSTRACT

This study examines the design and analysis of a training aircraft wing. The methodology includes aerodynamic and stress analyses. Microsoft Excel is utilized for scaling. Aerodynamic forces, load distribution, and air foil comparison computations were performed by Xflr 5. Inventor was used for stress analysis, which yielded wing deflections, Von Mises stresses, and safety factors. AutoCAD was employed to draw wing parts. The proper design for the cross-sectional shape of the inner wing components was determined. The goal is to find the lightest cross-section, the placements and numbers of wing ribs, and calculate the wing's dimensions. The findings revealed that wing tip deflection did not exceed 0.02. The von Mises calculations also show that the chosen material meets the requisite safety factor. For I and U sections, the deflection, von Mises stresses, and safety factor were 46.52mm and 43.27mm, 219.3 MPa and 152.7MPa, and 1.25 and 1.8, respectively.

@THIS IS AN OPEN ACCESS ARTICLE UNDER THE CC BY LICENSE:

<https://creativecommons.org/licenses/by/4.0/>



1. Introduction

Aircraft design is a process of iterative assumptions and calculations. Such estimates must be highly accurate. The conceptual design process provides a roadmap. Since aircraft performance is so critical to the mass, drag, and lift characteristics, it is relatively easy to make preliminary estimates. The wing is one of the basic structural components of the aircraft used to produce lift during flight due to the aerodynamic shape of the wing. In addition to Bernoulli's principle, the flow velocity is lower at the bottom and higher at the top of the wing. As a result, the pressure difference is created between both the wing's upper and lower surfaces, and thus, lift is generated. The wing must have a high strength-to-mass ratio and a high fatigue life because it is subjected to repeated alternating loads during flight [1].

Researchers (Usama Tariq & Farrukh Mazhar) studied the static structural analysis of aircraft. They updated the static structural analysis of wing beams, the methodology for researching fighter aircraft and determining critical, analytical, and numerical stresses for bending and tensile stress. The results obtained were analyzed using analytical calculations and numerical simulations. Bending, shear, and von Mises stress were calculated analytically and numerically for different loading conditions. The critical stresses were then formulated, and the wing beam's failure points or yield points were determined. Some of the simulated results in ANSYS exceeded the permissible limits under some loading conditions [2].

Vinoth Kumar & A. Waseem Basha, and others wanted to discuss the preliminary sizing and analysis of a trainer aircraft wing, focusing on structural optimization and stress analysis using classical engineering theories and FEA packages. The wing design is modeled in catiav5r20, and stress analysis is conducted using msc nastran/patran to determine the safety factor. Various loads and stresses during flight phases are considered, with a simplified approach treating the wing as a cantilever beam. The study concludes with an optimal wing design meeting strength and stability criteria, showcasing stress levels and deflections through FEA analysis [3].

In this scientific paper, Aerodynamic Analysis of wing design by understanding and analyzing the behavior of air around the wing, Modeling and analyzing the stresses that the wing is exposed to under different loads, such as aerodynamic forces and mass, integrating aerodynamic analysis and stress analysis by testing the results and using feedback to achieve an integrated and balanced wing design that combines both aerodynamic performance and structural load tolerance. The analysis of the cross-section results (I-Section) or (U-Section) were compared to find out which is better for the mass and calculating both von Mises

and deflection in the wing extension as well as the safety factor and knowing the weak points of the wing and ways to reduce these points and ways to prevent them. The programs (CATIAV5R21), (Inventor 2021), (AutoCAD 2021) and (xflr5_6.61) were used.

One of the gaps between researchers is that the cross-sectional shape of the beam (spar) has not been changed. However, some researchers have experimented with different cross-sectional shapes based on fatigue life [4]. In the current study, the cross-sectional shape of the beam (spar) was modified based on the results of the stress (von Mises), displacement, and safety factor analyses.

2. The Theoretical Bases

When designing a wing, several main tasks are required, including determining requirements, purpose, and operating conditions, as well as the mass of the aircraft during all stages of flight, sizing that weight, determining the wing cross-section, (airfoil), drawing the model, distributing loads, choosing the appropriate metal, and analyzing stresses.

2.1: Design requirements: Most of the values used for the calculations are based on the aircraft's general specifications, which can be seen in table (1).

Table 1. Specifications of the aircraft used [5]

General characteristics		
Crew	2	Airfoil NACA 64A012
Length	12.13 m	Range 1100 km
Wingspan	9.46 m	Thrust-to-weight ratio 0.37
Height	4.77 m	Wingloading 250 kg/m ²
Wing area	18.8 m ²	Mach number 0.8
Weight	3465 kg	Ceiling service 11000 m
Maximum take-off weight	4549 kg	Take off distance 530 m
power	14.7 kn	Landing distance 652m

2.2 Total take-off mass: The mass of an aircraft significantly influences its performance, safety, and efficiency. Take-off mass means the total mass of the aircraft, including passengers, cargo, fuel, and other necessary equipment for the flight. determining the take-off mass precisely is critical to ensure the safe takeoff and flight of the aircraft, as well as to enhance fuel consumption and performance. The main equations are [6].

The flight range (R), which can be found through the application of equation (1):

$$R = \frac{v}{c} * \frac{L}{D} * \ln \frac{w_i - 1}{w_i} \tag{1}$$

The gross weight or take-off weight is determined based on the following equation.

$$W_o = \frac{W_{crew} + W_{payload}}{1 - \left(\frac{W_f}{W_o}\right) - \left(\frac{W_e}{W_o}\right)} \quad (2)$$

The duration (E) of the maneuver can be calculated as demonstrated in equation (3):

$$E = \frac{L}{C} * \ln \frac{W_i - 1}{W_i} \quad (3)$$

Empty mass to total mass ratio ($\frac{W_e}{W_o}$) can be calculated using the equation (4):

$$\frac{W_e}{W_o} = A * W_o^{-c} * K_{vs} \quad (4)$$

The wet area (A_{wet}) can be calculated as defined in equation (5):

$$A_{wet} = \frac{A}{\frac{S_{wet}}{S_{ref}}} \quad (5)$$

The fuel to total mass ratio can be obtained using the equation (6):

$$\frac{w_f}{w_0} = 1.06(1 - \frac{w_n}{w_0}) \quad (6)$$

3. Sizing

Aircraft sizing determines the takeoff gross mass and fuel mass required for an aircraft concept to perform its design mission. A quick method based on minimal information about the design was used to estimate the sizing parameters. That sizing method was limited to fairly simple design missions [6].

The sizing process consists of four stages: calculating the landing distance to determine the maximum lift coefficient and maximum wing load relative to the take-off mass. The input values were entered using the excel program. The second stage involves the take-off distance, where the slope value is very low. Next, we find the thrust-to-mass ratio for take-off. The third stage addresses the rate of climb during the second part. The plane can take off again, but this differs from the previous case in which the thrust-to-mass ratio was determined for this stage. All the fundamental forces affecting the plane during flight also influence the glide ratio, which is a significant factor. The final stage examines the rate of climb during this phase as the plane approaches its destination. The same principle applies here, but it is adjusted by the landing mass ratio to take-off due to the landing stage. Finally, we calculate the horizontal flight stage and the thrust-to-weight ratio in horizontal flight. This culminates in the intersection of all the aforementioned stages, which detail how to calculate the wing load and thrust-to-mass ratio, linking the points through the various flight stages to achieve the lowest possible

thrust-to-mass ratio and the highest possible wing load, with each stage representing a specific line.

It is necessary to use a quick and easy method to estimate the first parameters through initial sizing in order to understand the meaning and effects of individual performance and configuration parameters. Loftin's method in 1980 was chosen due to its similarity to the characteristics of existing aircraft, by knowing the requirements at the airport and during the cruise [7].

3.1. Landing Distance: The first part includes various parameters and equations, such as landing distance, landing speed, and maximum lift coefficient for landing, in order to determine the maximum wing load to the take-off mass as eq. (7) [Ibid].

$$\frac{m_{MTO}}{S_w} = \frac{K_L \cdot \frac{\rho}{\rho_0} \cdot C_{L,max,l} \cdot S_{LFL}}{\frac{m_{ML}}{m_{MTO}}} \quad (7)$$

3.2. Take-off distance: The maximum takeoff lift coefficient is approximately 80% of the maximum landing lift coefficient. Today's aircraft have a maximum takeoff lift coefficient of approximately (2) as eq. (8) for detailed values.

$$\frac{T_{TO}}{m_{MTO.g}} = \frac{k_{TO}}{S_{TOFL} \cdot \frac{\rho}{\rho_0} \cdot C_{L,max,TO}} \quad (8)$$

3.3. Climb Rate during 2nd segment as eq. (9):

$$\frac{T_{TO}}{m_{MTO.g}} = \frac{N}{N-1} \cdot \frac{1}{L} + \sin \gamma \quad (9)$$

3.4. Missed approach as eq (10):

$$\frac{T_{TO}}{m_{MTO.g}} = \frac{N}{N-1} \cdot \frac{1}{L} + \sin \gamma) \cdot \frac{m_{ml}}{m_{MTO}} \quad (10)$$

4. Airfoil Selection

The airfoil section plays a crucial role in generating pressure for optimal distribution on the sides and bottom of the wing while minimizing aerodynamic cost (drag) in lifting the aircraft. For aircraft designers, having a fundamental understanding of aerodynamics and airfoil basics is essential for a standardized starting point. Testing the airfoil in a wind tunnel is a common practice, although it can be costly. However, there are programs available to test and select the best airfoil. figure. (2) illustrates several geometric parameters of a typical airfoil section [6].

The steps to choose the best (air foil) [8]:

1. Equation to determine the average weight (W_{vag}) of the aircraft during the flight

$$W_{avg} = \frac{1}{2}(W_i + W_f) \quad (11)$$

2. Calculating the ideal flight (C_{ic}) lift coefficient for the aircraft by:

$$C_{ic} = \frac{2W_{ave}}{\rho V_c^2 S} \quad (12)$$

3. Equation for wing lift coefficient (C_{LCW}) is

$$C_{LCW} = \frac{C_L}{0.95} \quad (13)$$

4. Calculating the ideal airfoil lift (C_{LI}) coefficient by:

$$C_{LI} = \frac{C_{LCW}}{0.9} \quad (14)$$

5. Calculating the maximum lift coefficient (C_{lmax}) of the aircraft by:

$$C_{lmax} = \frac{W_{To}}{\rho V_c^2 S} \quad (15)$$

6. The equation for calculating the wing's maximum lift coefficient is (C_{Lmax_w})

$$C_{Lmax_w} = \frac{C_{Lmax}}{0.95} \quad (16)$$

Calculate the total maximum lift coefficient of the airfoil. Find from the above equations (11-16) the ideal lift coefficient for flight and the total maximum lift coefficient. Drop the points in figure (1) and determine three wings as a minimum.

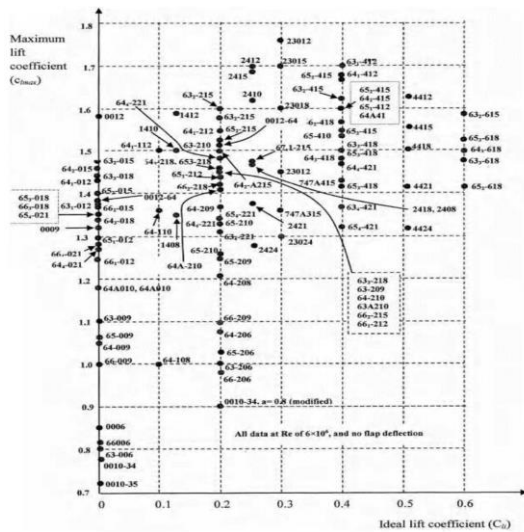


Figure 1. Maximum lift coefficient with optimal lift coefficient [8].

5. Load Distribution Calculations

The load distribution on the wing is calculated using the (Xflr5) program, based on the speed setting and using the (Ring vortex) analysis method at the angle of attack (5°) in the case of horizontal flight. In addition, the angle of attack is modified to (4.38°) to calculate the load distribution accurately by making changes to the data and correctly finding the appropriate angle of attack.

After analysis, it is easy to find the diagram of the relationship between the lift coefficient and the wing span or the positional lift and the wing span. By doing so, the relationship between the load and the wing span (y-span) can be found, meaning the distribution of the load on one of the wings. The equations can be used to [6].

$$local\ Lift(l) = \frac{CL * Chord}{MAC} \quad (17)$$

$$Load = local\ Lift * v^2 * \rho / 2 \quad (18)$$

6. Drawing The Models

1. Drawing the prototype of the designed wing (2D) and determining the dimensions and length: The dimensions were drawn from theoretical calculations, as shown in figure 2.

2. The airfoil consists of many points. These points are determined via the Airfoil tools website, and then you use the catia program to draw the airfoil as in figure 3.

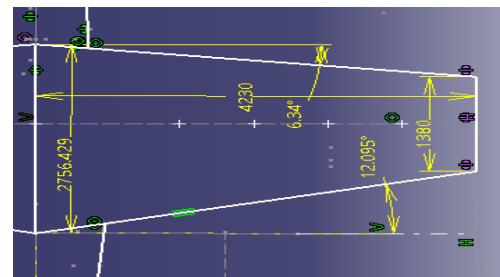


Figure 2. Determining the wing dimensions using catia software

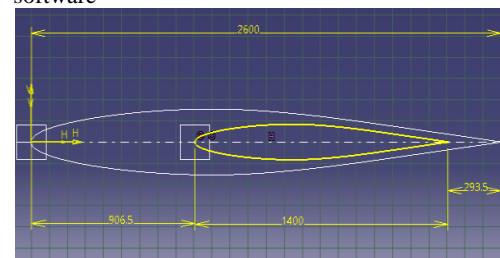


Figure 3. Drawing the airfoil using catia software

3. Skin drawing: First, the airfoil (Air foil) is transferred to the program (AutoCAD 2021) from the side of the fuselage (root) and the far side (tip). Thus, we have two winglets on the side of the fuselage and the far side. Then, each winglet is dismantled, and parallel lines (offset) are made. Its size is (2mm) for each winglet, as shown in figure 4.

4. One of the wings consists of eight sides with unequal distances, as shown in figure. (4). Wing divisions are based on the load distributed according to previous studies and only

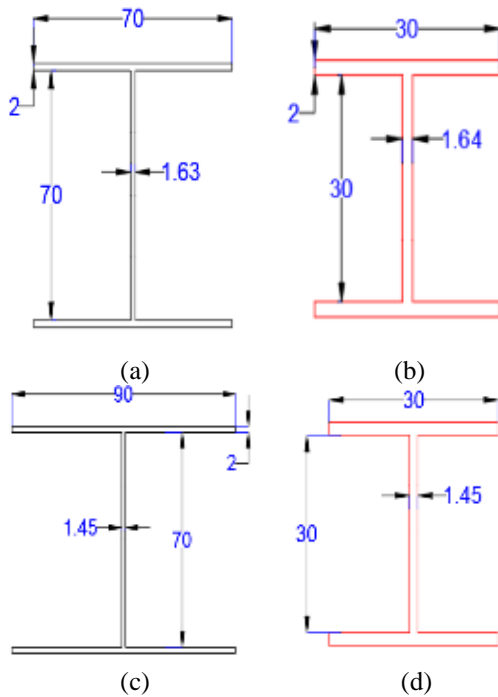


Figure 5. (a) dimensions of rear spar tip (mm), (b) Dimensions of rear spar (mm), (c) Dimensions of front spar tip (mm), (d) Dimensions of front spar tip (mm).

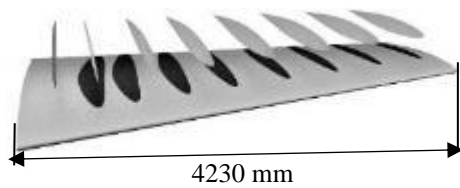


Figure 4. Ribs distribution diagram for the designed wing

5. The shape of the front crossbar is (I-section) from the side of the fuselage (root). It will be at a distance of (0.25) from the length of the airfoil (chord), as the dimensions were taken from a reference according to the best value for the span design, where the thickness and the full weight of the incident mass was (62.5 kg), as shown in figure 5a.

5.1- The shape of the front crossbar is (I-section) on the far side of the plane (tip). The far side of the plane is also for the blank. The crossbar is at a distance of (0.25). The front crossbar and the successor crossbar are at the same previous dimension, but the dimensions differ for the section (I-Section) due to the length of the (Airfoil chord), where the thickness is fixed (2mm flange), as shown in figure 5b.

6- The shape of the successor crossbar is (I-section) from the side of the fuselage (Root). It is at a distance of (0.62) from the length of the airfoil

(chord), The mass of the (I-section) was (56.5 kg), figure 5c.

6.1 The shape of the successor crossbar is (I-section) the far side of the plane (tip). It is at a distance of (0.62) from the length of the airfoil (chord) .The weight of the canopy was (56.5 kg), as shown in figure 5d

7. Drawing the front and rear crossbars (span) of the half wing It is an extension of the crossbar along half the wing, in the first case without holes or in the second case with holes to reduce weight in figure 6.

8. Assemble the parts: skin, ribs, and span. where the mass of the half wing was (121 kg) and the mass of the full wing was (242 kg) in figure 7.

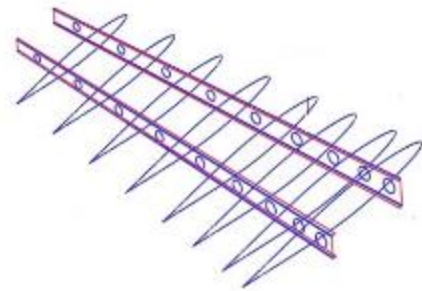


Figure 6. Illustrates the assembly of both ribs and spars

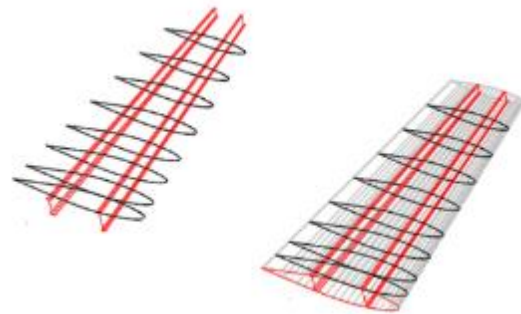


Figure 7. Assembly of both ribs, skin, and spars

9. The last process is perforating the beam (span) as fig. (8)(9) [6]:

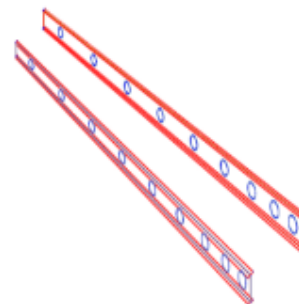


Figure 8. Illustrates the perforation of the spars

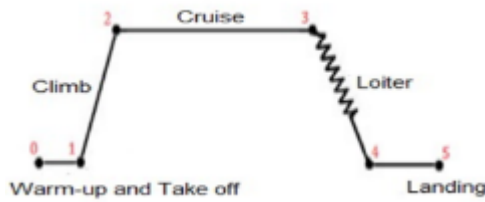


Figure 10. Overview of the mission plan [11]

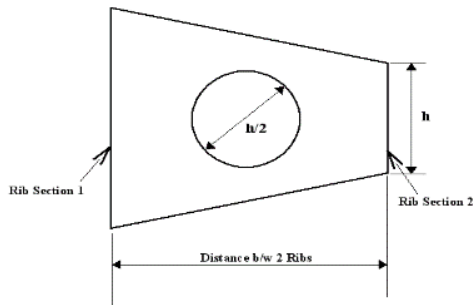


Figure 9. Describes how the piercing process occurs [6]

The dimensions are taken according to the reference [6], where the weight of the front keel after the hole is (58.5 kg) and the mass of the rear keel is (53kg), and the weight difference was approximately (8 kg) depending on the length of the wing.

7. Choose Material

Aluminum alloys are commonly used in modern aircraft construction. They are valuable because they have a high strength-to-mass ratio. Aluminum alloy is corrosion-resistant and relatively easy to manufacture. The distinctive feature of aluminum is its weight.

The alloy (aluminum 2024 -T3) is used in the fuselage and lower wing skins, which are susceptible to fatigue due to applications of cyclic tensile stresses. For upper-wing skins subjected to compressive stresses, fatigue is less of a problem. Aluminum alloy. They are 10% stiffer, 10% lighter, and have superior fatigue performance [9]. Therefore, the alloy 2024-T3 was chosen, as shown in table 2.

Table 2. properties of alloy (aluminum 2024-T3) [10]

Properties	Value	Properties	Value
ultimate Strength	483MPa	Density (ρ)	2780 kg/m ³
yield Strength	385MPa	Young's Modulus, (E)	73.1GPa
shear Strength	283MPa	Shear Modulus, (G)	28Gpa
Poisson' Raito, (ν)	0.33		

8. Results and Discussions

8.1. mass results: The amount of fuel in an aircraft is a major factor in determining how far the aircraft can reach and complete flights safely, at each stage as in figure (10) and without problems. The results of each stage of the fuel are shown in table (3). Table (3) shows the fuel consumption results at each stage of the flight.

Table 3. fuel consumption at each stage

Segment	w_f (kg)	WF
0-1	1239	W1
1-2	1220	W2
2-3	1086	W3
3-4	960	W5
4-5	955	W6

Mass results from the above equations (1-6): Find the take-off weight (4783.747 kg), empty weight (3013.76 kg), crew weight (200kg) , payload weight (293kg), and fuel weight. (1277kg). These guesses are the initial results of the mass. My results show a high degree of agreement with those of [12], strengthening the model's validity.

8.2. sizing results: The final result is shown in figure (11) that the values are reasonable according to the aircraft specifications and the required space, as the load was (245 kg/m²), where the estimated area can be found at (19.18 m²), which is the closest thing to the designed wing space and achieving the sizing goal.

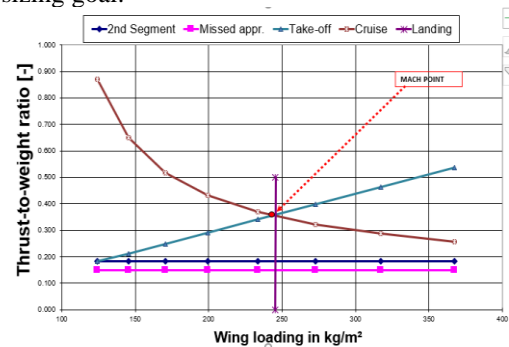


Figure 11. Design space through sizing process.

Results after sizing: Take-off weight increased by (1%), landing mass increased by (2%), fuel mass increased by (1.4%), and empty mass increased by (1%).as the table (4)

Table 4. shows weight results after sizing

Max. Take-off mass	m_{MTO}	4756
Max. landing mass	m_{ML}	3893
Operating empty mass	m_{OE}	2991
Mission fuel fraction	m_F	914
Wing area	S_W	19 m ²

The specifications of the aircraft close to the design used (Aero L-39 Albatros) show the values of the results and the extent of convergence between the results after scaling, where we notice from table (5) slight differences in mass. This is because there are inputs related to the aircraft specifications that cannot be accessed in a precise manner. For example, the mass of the fuel cannot be estimated accurately because it depends on several factors related to the type of flight, so it was entered speculatively. Primary data similar to those used by the researcher [12] were used, allowing for comparison of results. Table (5) comparison of sizing results and aircraft specifications L-39C “albatros”

8.3. Airfoil selection:

Compare the three (airfoil) as shown in figure (12) will notice from the drawing that there is a symmetrical airfoil or an asymmetrical airfoil, where the symmetrical one (naca64-012A) does not generate lift at zero angles and (naca 2424) is asymmetrical as it generates lift at zero angles, as well as (naca63-221). Whereas asymmetrical generates higher lift at an angle of (15-20) degrees and the lift ratio are 1.49, or symmetrical does not generate high lift between an angle of approximately (10-13) degrees where the lift ratio is (1.25), but is relatively stable, but (naca63-221) generates moderate lift. Relatively (7-15), and the leverage ratio is approximately (1).

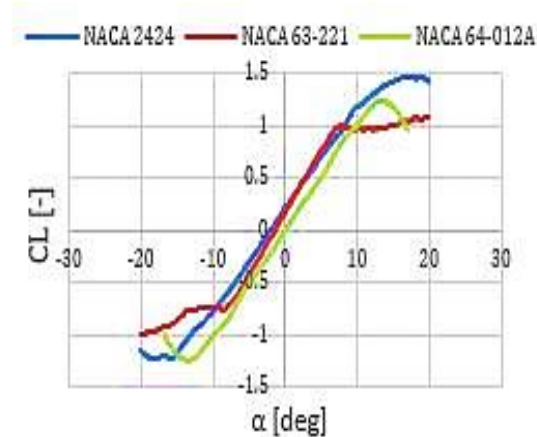


Figure 12. angle of attack Vs lift [Xflr5].

In terms of properties, asymmetrical is better, but it generates higher drag, which means better properties but more problems, as shown in figure (13). for the symmetrical airfoil (naca 64-012A), the drag ratio is slightly less, about (0.01). For the other airfoils (naca 63-221), the drag ratio is about (0.01), which is undesirable for airfoils.

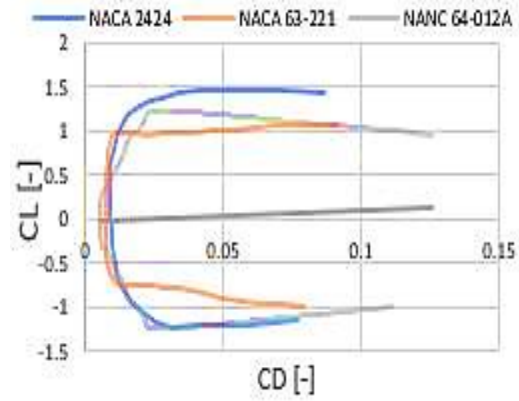


Figure 13. Coefficient of lift Vs drag [Xflr5].

Table 5. comparison of sizing results and aircraft specifications L-39C “albatros”.

weights and area	(M)kg	aircraft specifications	Mass after sizing
Takeoff mass	M_{MTO}	4700	4756
Landing mass	M_{ml}	3915	3893
Empty mass	M_e	3455	2991
Fuel mass	M_f	980	914
Maximum Load	m_{MTO}/S_w	$250\text{kg}/\text{m}^3$	$245\text{kg}/\text{m}^3$
Thrust to mass Ratio	$\frac{T_{TO}/(m_{MTO} \cdot g)}{m_{MTO}/S_w}$	0.37	0.359
Wing Area	S_w	18.8m^2	19m^2

For the other airfoils (naca 2424), the drag ratio is greater. (0.012) and this is not desirable for airfoils. We also note that for the symmetrical airfoil (naca 64-012A), there is a very clear benefit that the drag ratio is constant when raised from (0- 0.3) according to it, and negative is therefore chosen among the airfoils. And also, for the airfoil (naca 63- 221) When Lift (0-1) Airfoil (naca2424) at lift (0-1.25) as fig. (13). Researchers Stein, H. J., and others also compared the airfoils and chose the best one. The maximum lift coefficient for the same airfoil type was very close to the researchers, indicating the validity of the calculations and comparisons [14].

8.4- distributing loads:

Distribution of local lift with wing span (y-span) at an angle of attack (4.38°) in horizontal flight. A high lift coefficient starts at the root of the fuselage and then gradually decreases to a lower lift coefficient at the far wing tip, as shown in figure (14).

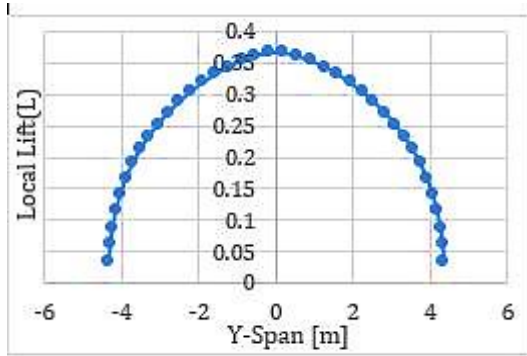


Figure 14. The distribution of local lift with wing span is shown [Xflr5].

Table 6. Load distribution values on the wing

Tip	section on the wing (y)	chord length(c)	shear force of each section
Root			
NO	(m)	(m)	(kn)
1	4.23	1.4	0.642
2	3.957	1.475	1.106
3	3.411	1.55	1.678
4	3.138	1.625	1.846
5	2.865	1.70	1.970
6	2.592	1.775	2.067
7	2.319	1.85	2.153
8	2.046	1.925	2.237
9	1.773	2.0	2.324
10	1.5	2.075	2.415
11	1.275	2.15	2.489
12	1.05	2.225	2.559
13	0.825	2.30	2.617
14	0.6	2.375	2.654
15	0.45	2.450	2.662
16	0.3	2.525	2.652
17	0.15	2.60	2.620

Where the relationship between the positional lift (L) and the wing span (y-span) according to the program (xflr5) is divided into unknown distances, but it can be used to find the load distributed on one of the wings from equation (17) and (18) from equation (18), the load can be calculated as distributed but at unknown distances, but specific distances are required between the ribs (Ribs) according to the wing design so that the load can be applied accurately.

$$l = -34.8y^4 + 261.88y^3 - 709.19y^2 + 494.23y + 2561.7 \quad (19)$$

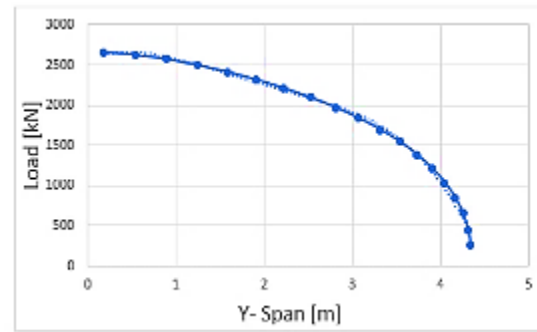


Figure 15. shows the distribution of the load on the (y-Span) [Xflr5].

figure (15) shows the relationship between the load (Load) and the span of one of the wings (Y-Span) or (Chord) distributed according to unknown distances, but an equation was formed linking the load and the wing span by defining the curve and choosing a polynomial system and its fourth order and showing the equation, to facilitate the process of finding the load at each point according to each section where the value (y) represents the distances between the sections. For example, (y1) is the distance from the root of the aircraft body to the tip of the wing to get (17) pieces, as shown in fig. (16)

And also (y2) (y17) until the distance becomes zero to produce the load values (L1) (L17), as shown in figure (16), shows how to calculate the load distribution on a wing to produce the values in table (6), which shows load distribution values on one of the wings.

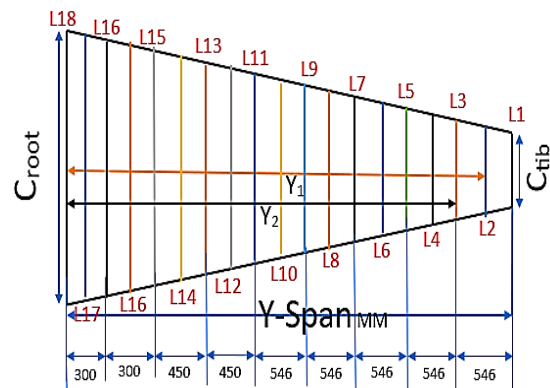


Figure 16. Explains how to calculate load distribution.

The xfoil program was used to simulate the airflow and analyze the aerodynamic performance of the wing, in addition to using matlae to perform the calculations and data analysis. The results of the two programs were compared using the same input data and geometric dimensions of the wing. The comparison between the results extracted from MATLAB and xfoiil showed a clear convergence, reflecting the accuracy of the computational and simulation models used in this research. This convergence is clearly shown in figure (17), as the

results indicate a significant overlap between the calculated and simulated values.

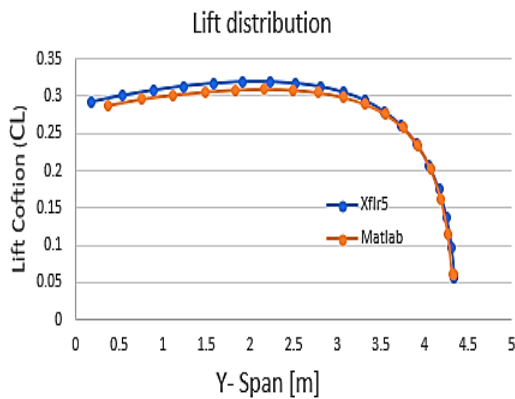


Figure 17. Shows a comparison of results with two programs (MATLAB and xflr5).

8.5 - Cantilever analysis of one of the wings with holes in the crossbars:

Analyzing the model Static analysis of a wing is an essential step in the design and development process of an aircraft. It involves analyzing the wing's behavior under static loading conditions, which includes the weight of the aircraft, payload, and other external loads. fixed support root rib Force is applied to each rib in the order (0.642 to 2.620) kn, starting from root to tip, respectively, as shown in table (6).

Analysis of one of the wings, after applying the load to it vertically, distributed according to the sides, and determining the value of the loads according to the load distribution calculations on the wing, then applying the forces using the (Inventor2021) program, and the wing is drawn using the (Auto-CAD 2021 - English) program.

We note from figure (18a) the analysis of the wing structure with holes in the two spar beams and the displacement value of 46.52mm to the holes in the beam that reduce the weight and increase the deflection.

figure(18c) shows the stress(von-Mises), which was 219.3 MPa less than the case without holes by 37.95%, which is less than the yield strength of aluminum alloy 2024-(T3), and it proves that the structure is safe because the amount of stress gained from the analysis is less than the yield strength of the structural material. Also, the safety factor of 1.25 is greater than the case without holes by 38.4%, which proves that the wing structure has been improved and out of the danger zone.

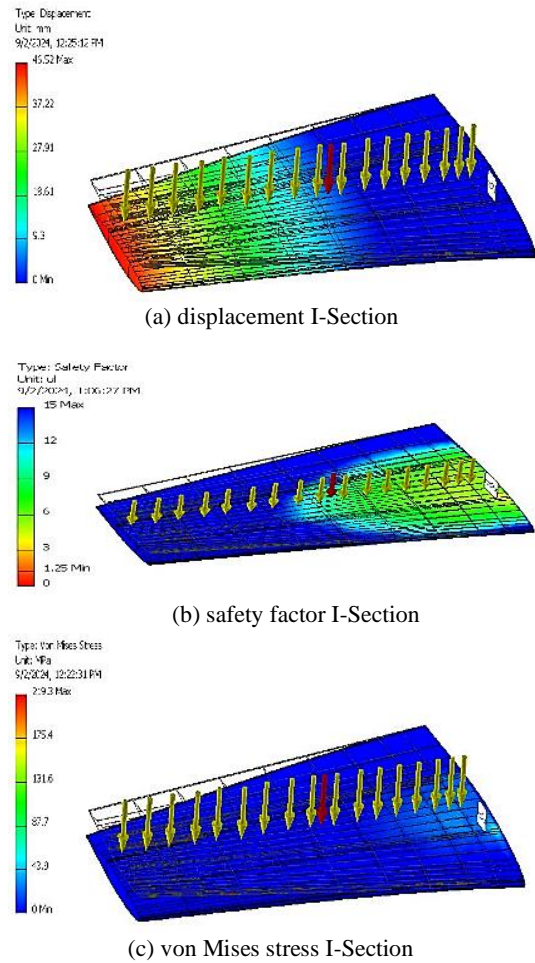


Figure 18. (a) displacement & (b) safety factor & (c) von Mises stress.

8.5.1 -Analysis of the wing by changing the section from (I-Section) to (U-Section):

figure (19a) shows the analysis of the wing by changing the section from ((I-Section to (U-Section) and the displacement value was 43.27 mm, which decreased by 7% compared to the second case, but with an increase in weight of 10 kg due to a change in the shape of the cross-section (I-Section) to ((U-Section). figure (19c) shows the stress (von-Mises), which was 152.7 MPa less than the first case by 69.63%, which is less than the yield strength of aluminum alloy 2024-(T3), and proves that the structure is safe because the amount of stress obtained from the analysis is very less than the yield strength of the structural material. Also, figure (19b) shows the safety factor by 1.8 greater than the first case by 69.44%, which indicates the success of converting the section from (I-Section) to (U-Section). Also, the load factor ((n=1 and (n=2) can be used to ensure flight stability.

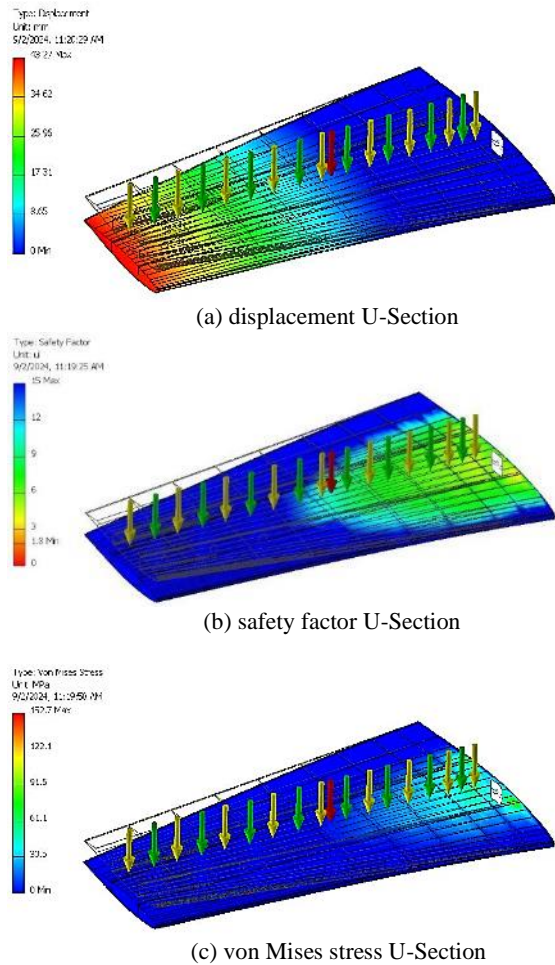


Figure 19. (a) displacement & (b) safety factor & (c) von Mises stress

9. Conclusions

The current study paper concludes that the weight of each stage of flight is displayed, in addition to the relationships between net weight. The purpose of this is to know the effect of each factor and its danger with weight. The second step is sizing the flight stages, achieving the goal, and comparing it with the designed aircraft's data to ensure the results' accuracy. The third step is to choose the appropriate airfoil that the designed model is suitable for working, according to previous studies, and that (U-Section) is better than (I-Section) but has a higher weight that should be considered.

10. Comparison Study

The results obtained in the current research were compared with the results of the researchers Ibtisam and Mr. Gargan [15,16], who used the same wing design and material, showing the stress (von-Mises) (361Mpa) and displacement (47mm), and compared with the displacement obtained (43.27mm) for the U-Section and I-Section, along with von Mises stresses of 219.3 MPa and 152.7 MPa and masses of 226 kg and 264 kg, respectively. This is evidence of the validity of the results. Mr. Gargan [16]

Skin thickness (mm)	Displacement (m)	von Mises stress (MPa)	Mass (kg)
1.5	0.056	460	414
2	0.047	361	440
2.5	0.041	298	467

List of symbols

S.NO	SYMBOLS	PARAMETERS
1	C	Chord (m)
2	V, u	Velocity (m/s)
3	W/S	Wing loading (kg/m ²)
6	E	Endurance (s)
7	R	Range (km)
9	S	Wing area (m)
10	L	Lift of aircraft (N)
11	We	Empty mass(kg)
12	Wf	mass of fuel (kg)
13	Wc	Overall mass (kg)
15	CD	Drag coefficient
16	CL	Coefficient of lift
17	L/D	lift-to-drag ratio
18	Awet	Aspect ratio wet
19	A	Aspect ratio
20	N	Number of engines
21	S _{FL}	Landing distance (m)
22	ρ/ρ0	Density ratio
23	MAC	Mean aerodynamic chord (m)
24	W _{crew}	Crew mass (kg)
25	W _{payload}	Payload mass (kg)
26	W _i	Mass at each flight stage
27	K _{us}	Constant
28	S _{wet}	Wet area (m ²)
29	S _{ref}	Reference area (m ²)
30	m _{MTO}	Mass at takeoff (kg)
31	K _L	constant factor
32	ρ	Density
33	ρ0	Air density
34	C _{L,max,l}	Maximum lift coefficient Airfoil
35	m _{ML}	landing mass (kg)
36	S _w	Wing area (m ²)
37	T _{TO}	Thrust on takeoff
38	G	Gravitation (9.81)
39	N	Number of engines
40	w _n	The final stage mass

Acknowledgements

This research was financially supported by the mechanical engineering department at the College of engineering / Mosul University.

References

[1] M. Ragamshetty, T. Sai Deepthi, V. Anil, T. Akhil, A. Shiva " Design and Finite Element Analysis of Aircraft Wing," International Journal of Research Publication and Reviews, vol. 3, no. 7, pp. 995-1006, 2022.

[2] U. Tariq, F. Mazhar, " Static Structural Analysis of Fighter Aircraft's Wing Spars" International Bhuban Conference on Applied Sciences & Technology , vol. 4, no. 22, pp. 221-243, 2021.

[3] T.S.Vinoth kumar, A.Waseem Basha, M.pavithra, V.Srilekha, " Static & Dynamic Analysis of Atypical Aircraft Wing Structure Using MSc Nastran" International Journal of Research In Aeronautical And Mechanical Engineering, vol.3, no. 8, pp.1-12 , 2015.

[4] K. Eldwaiba, A. Grbovića, G. Kastratovićb, M. Aldarwisha, " Design of Wing Spar Cross Section for Optimum Fatigue Life", Vol. 4,no. 7,pp.1-6, 2018

- [5] Othman and M. Al-Obaidi , "Effect of the wing airfoil shape on the aerodynamics and performance of a jet-trainer aircraft – An optimization approach", *Journal of Physics: Conference Series*, vol.8, no. 12, pp.1-12, 2021.
- [6] D. Raymer, "Aircraft Design: A Conceptual Approach", American Institute of Aeronautics and Astronautics, Washington, U S A, 1992.
- [7] M. Krull "Preliminary Sizing of Propeller Aircraft (Part 25)", M.S. thesis, Dept. of Automotive and Aeronautical Engineering, Hamburg University of Applied Science, Germany, ,2022.
- [8] M. Sadraey, "Aircraft Design a Systems Engineering Approach," Chapter 5: Wing Design, USA, 1992
- [9] F. H. Darwisha, G. M. Atmehb, Z. F. Hasanc, , " Design Analysis and Modeling of a General Aviation Aircraft", *Jordan Journal of Mechanical and Industrial Engineering*, vol.6,no.2,pp.183–191, 2012.
- [10] T. Kebir and others, "Simulation of fatigue damage under variable loading", *Journal Structures Development Durable*, vol. 17, no. 9, pp. 1-14, 2019.
- [11] A. Badis, "Subsonic Aircraft Wing Conceptual Design Synthesis and Analysis", *International Journal of Sciences: Basic and Applied Research (IJSBAR)*, vol. 35, no 3, pp. 64-108, 2017.
- [12] Royd A. Johansen, " Conceptual Design for a Supersonic Advanced Military Trainer", M.Sc. thesis, Faculty of Aeronautics and Astronautics Engineering, San José State University, Washington, USA, May 2019.
- [13] Jimi S immons , " Aero L-39C Albatros ", U SA H , vol. 4, no. 56, pp. 1-7, 2020.
- [14] Stein, H. J., Picraux, S. T. , Holloway, P. H., " Effect of the wing airfoil shape on the aerodynamics and performance of a jet-trainer aircraft - An optimization approach", *Journal of Physics: Conference Series*, vol. 2120, no 1,pp.12 , December 2021.
- [15] Ibtisam J. Ismael, " An Optimum Design of a Subsonic Aircraft Wing due to the Aerodynamic Loading", *The Scientific World Journal Volume* vol.4, no. 6, pp.1-13, 2024.
- [16] M. Gargan, "The optimum structural design of aircraft wing by using finite element method," M.S. thesis, Dept. of Machinery and Equipment Engineering, University of Technology, Baghdad, Iraq, 2001.